Precise Modeling of High Impedance Faults in Power Distribution System in EMTPWorks Software

M. Jannati[1], **L. Eslami**[1]
[1] Electrical Engineering Department, University of Kurdistan, Sannandaj, Iran
Email: Mohsen.Jannati@gmail.com

Abstract: *In all distribution networks, commonly it is possible for energized conductors to come into contact with the outside substances like trees, building walls and also surfaces below them. This condition, known as high impedance fault, is very dangerous for human life and may result in electricity congestion, burning or ignition by the arc or the substance heat. In addition, a part of the energy produced by the power company is lost and this loss causes damage in power supply plants. Traditional relaying in distribution networks only detects short circuit situations and thus very considerable amount of generated electric power flows through the earth without achieving by the load. Because the occurrence of the high impedance fault is accompanied by very small increase in load current, it is very difficult for protection relays to identify it. For extracting a precise and appropriate method for HIF identification, it's necessary to model high impedance fault arc. Therefore, this paper explains how to simulate high impedance faults in distribution systems. At first various modeling of this faults is given and then a precise improved model has been presented. Also the simulation method of this model in EMTPWorks environment has been explained completely.*

Keywords: *High Impedance Fault; Precise Modeling; EMTPWorks;*

1. Introduction

High Impedance Fault (HIF) is defined as an electric connection between an energized conductor and an external dielectric substance [1]. Dielectric substances only transmit limited value of current through themselves, because their resistance is inherently great [2]. So, when a HIF happens, it is not identified as an abnormal situation by the traditional protection equipments. Actually, a current with very low amplitude from the energized conductor flows to the earth via the connected substances ignoring how the connection has been established [3]. This current flows into the earth having very high potential that may harm people.

When the conductors in the distribution network come into contact with the foliage, earth surface and concrete walls, common type of HIF occurs [4]-[6]. These situations usually exist around the conductors in overhead distribution system lines. In Fig. 1, a distribution system has been shown with its conductors which are prone to contact with foliage.

In contrast to the other kinds fault that cause high amplitude current, the amplitude of current in HIF is very low [7]. So, the traditional protection equipments similar to the over current protection cannot recognize this type of fault. Unsuccessful detection of HIF can happen human damages or lead to ignition [8]-[10].

Therefore for extracting a precise and appropriate method for HIF identification, it's necessary to model HIF (HIF arc). Precise simulation results can be achieved by precise modeling. So, in this paper HIF modeling methods are reviewed at first and then the best model is selected and its imperfections are corrected. Finally, the modeling method of proposed model is explained in EMTPWorks software.

The rest of the paper is organized as follows: In section 2 different HIF arc models is explained. Proposed dynamic model of HIF arc has been presented in section 3. In section 4 implementation of HIF arc modeling in EMTPWorks is explained step-by-step. Section 5 provides introducing of under-study distribution network. Also, simulation results are presented in section 6. Section 7 draws the conclusion and finally the references are presented at the end of the paper.

Fig. 1 Connection probability among conductors and foliage.

2. HIF Models

In 1985 the first model for HIF was proposed by connecting a resistance to the system at the fault location [11]. Considering the experiments performed by Emanuel in 1990, a model for HIF was proposed based on the sparks nature when the conductor comes into contact with the ground [12]. This model has been formed from two DC power supplies and two diodes paralleled each other inversely. Likewise a resistance and a reactance control the amplitude and current of the fault. This model has been shown in Fig. 2.

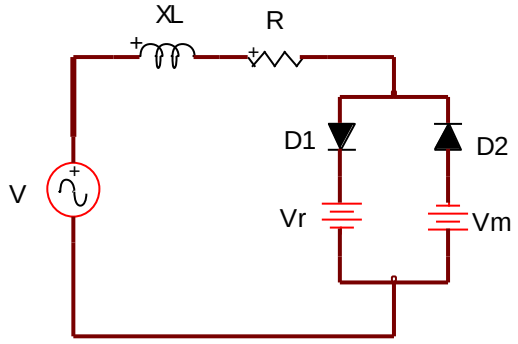

Fig. 2 Emanuel model for HIF.

In 1993, this resistance and the reactance were replaced with two nonlinear resistances (according to Fig. 3) to consider the nonlinear behavior of the ground in some way [13].

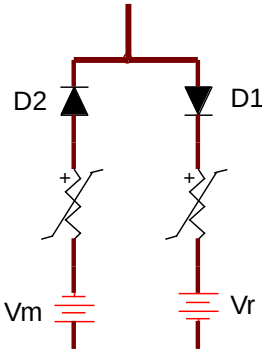

Fig.3 HIF model presented in 1993.

A model formed of nonlinear impedance, time variable voltage power supplies and TACS (Transient Analysis of Control System) control switches was introduced in 1996 that has been shown in Fig. 4 [14].

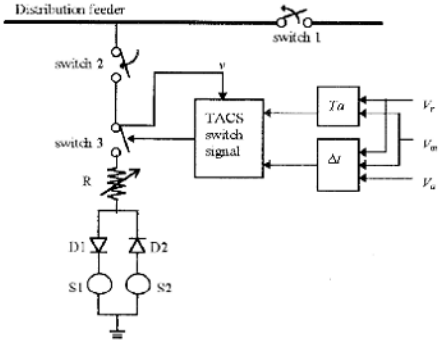

Fig.4 HIF model with considering the arc characteristic [14].

A HIF model by using two series nonlinear resistance shown in Fig. 5 was presented in 2001. One of the resistances models nonlinearity and asymmetry of fault current and another shows transient in time of fault occurrence [15].

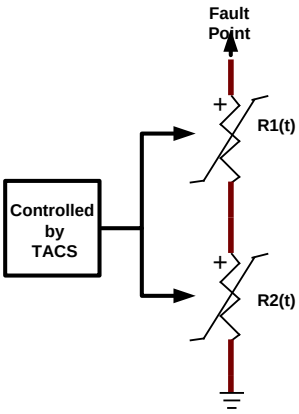

Fig. 5 HIF model by using two nonlinear resistances.

In 2003, to produce HIF current the model in Fig. 6 was used in which Rp and Rn model fault resistances. Also for modeling asymmetry of current, resistances were considered different [16].

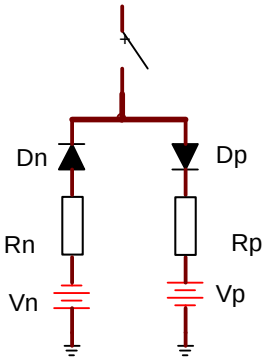

Fig. 6 HIF model presented in 2003.

HIF model in Fig. 7 including a nonlinear resistance, two diodes and two DC sources with amplitudes which change in every half cycle randomly has been presented in 2004. Average changing and variance of DC voltage source amplitude were determined related to the type of earth surface [17].

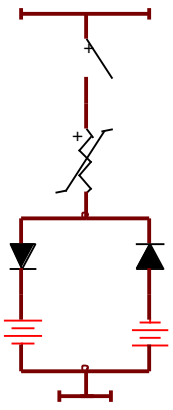

Fig. 7 HIF model by using nonlinear resistance and Changing DC sources.

In 2005, another HIF model according to Fig. 8 has

been introduced. In this model linear resistance R(t) is ground equivalent resistance, r(t) is arc dynamic state and DC and AC sources model asymmetry of fault current, and quenching alterations of arcs respectively [18].

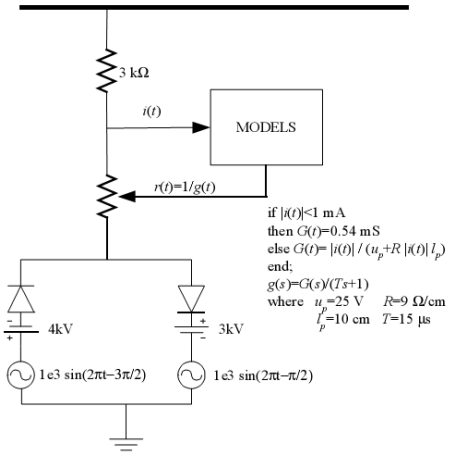

Fig. 8 HIF model presented in 2005 [18].

According to Fig. 9, a nonlinear resistance controlled by EMTP models has been introduced as an arc model In 2006 [19].

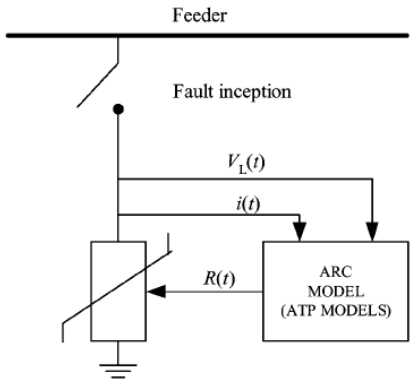

Fig. 9 HIF model by using EMTP models [19].

In 2007 a HIF model was presented by N. Elkalashy et al in [20] which is more precise and more complete comparing with the other available ones. However, in the simulations of this model the arc behavior in two positive and negative half cycles has been considered the same for convenience. So in this paper, completely precise modeling has been present in EMTPWorks. The modeling procedure is explained step-by-step. It is evident that precise modeling leads to more precise simulation results and extracting a more comprehensive method.

3. HIF Arc Dynamic Model

An experiment has been done to measure the characteristic of a HIF happening in a 20 kV distribution network in [20]. This experiment has two parts which the first one is determining the tree resistance and the second part is attaining the characteristic of HIF fault. To observe the experiment circuit and execution process of each part refer to [20].

Voltage and current of the fault occurring in three different locations including leaves, branch and trunk of a tree have been shown in Fig. 10. It is observed that if the fault happens because of connecting the conductor to the tree leaves, the arc is suddenly quenched once the fault current crosses the zero point. When the fault voltage increases in fault point, the arc will be established again. Fig. 10.a shows the magnified diagram of this phenomenon.

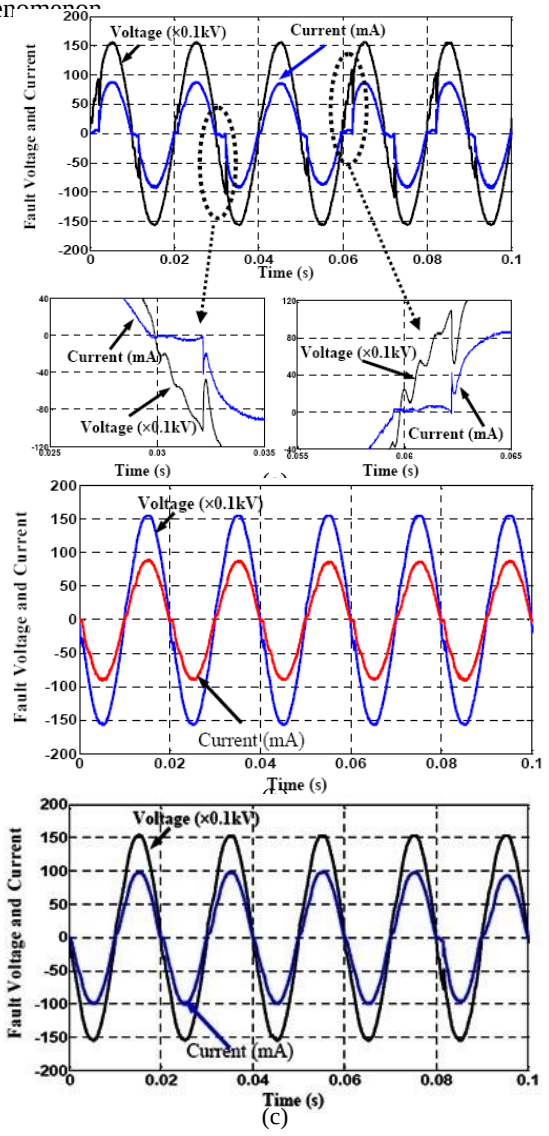

Fig. 10 Voltage and current waveforms (a) when fault happens in the leaves of a tree (b) when fault happens in the branches of a tree (c) when fault happens in the trunk of a tree [20].

Fig. 11 shows the voltage-current characteristic of tested HIF current for Fig. 10.a. As seen, HIF arc behavior is different in two positive and negative half cycles. However, a model in which arc voltage- current characteristic in two half cycles is different as in experimental results has been proposed in this paper.

The comprehensive model which is used to describe arc in [20]. In this model, equation (1) is used based on thermal equations in order to determine the changeable arc conductance:

$$\frac{dg}{dt} = \frac{1}{\tau}(G - g) \qquad (1)$$

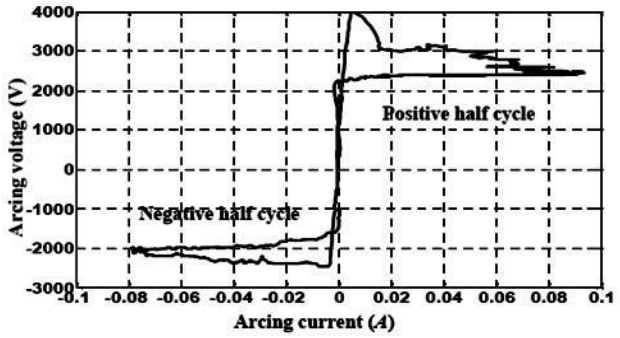

Fig.11 Experimental voltage-current characteristic of HIF arc [20].

Where, g is time variable conductivity of arc, $G = |i| / V_{arc}$ is the stationary arc conductance, $|i|$ is the absolute value of arcing current, V_{arc} is a constant value of arcing voltage and τ is the arc time constant. All the above parameters are determined in a way that the results will be the same as the experimental results.

The characteristic shown in Fig. 11 is used to calculate these parameters. Moreover, equation (2) is used to calculate τ :

$$\tau = Ae^{Bg} \qquad (2)$$

Where A, B are constants and similar to V_{arc} have different values in two positive and negative half cycles of fault voltage and current which could be estimated by the experimental results. The values of positive half cycle are:

$V_{arc} = 2520V$, $A = 6.6E-5$ and $B = 41977$ in [20]. For the negative half cycle the values are:

$V_{arc} = 2100V$, $A = 2.0E-5$ and $B = 85970.30$. Indeed all these values are calculated for Fig. 10.a.

General dynamic model of arc denoted as a HIF element in Fig. 12, has been shown in Fig. 13. To simulate this experiment, a network similar to the test circuit shown in Fig. 13, is used in EMTPWorks software. The arc dynamic model shown in this circuit is derived from the above equations and will be detailed in following. Note that input values of this circuit are used to obtain waveforms of Fig. 10.a.

In Fig. 14, CTR control signal used for controlling the controllable integrator in Fig. 12 has been shown. Indeed, this part of model indicates the arc sudden quenching when the current is crossing zero point. The integrator output is calculated by integrating the main input until the control signal is high, and once it turns to low, the integrator output will be RES signal. Actually, RES signal gives the arc resistance at quenching moment. Based on the experimental results, resistance value is a time variable function with a slope of $0.5M\Omega/ms$ through the first 1ms interval after the arc quenching, and $4M\Omega/ms$ after 1ms. Thus, the sudden quenching and reigniting of arc can be simulated using the CTR signal acquired by the results of Fig. 10.a [21].

4. HIF Arc Modeling in EMTPWorks

Considering Fig. 12, it is clear that in order to implement the model in EMTPWorks, the absolute value

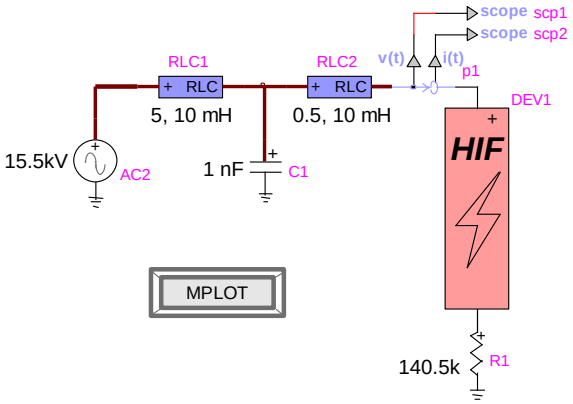

Fig. 12 Network used for HIF modeling in EMTPWorks.

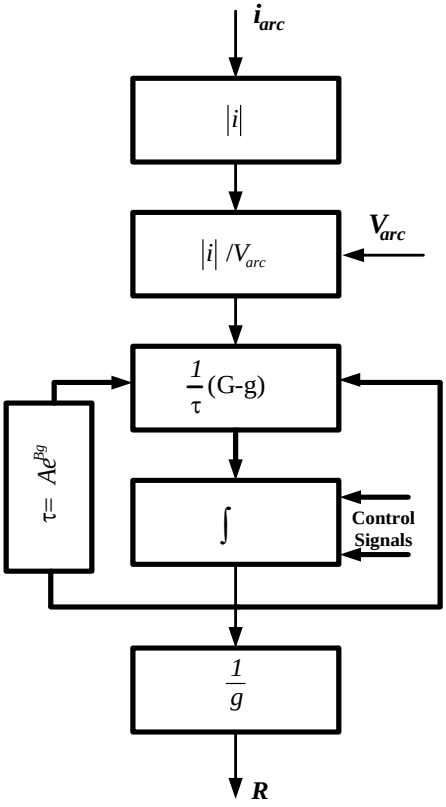

Fig. 13 Arc comprehensive model in HIF.

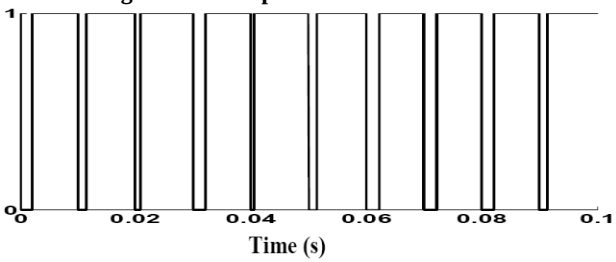

Fig. 14 Control signal used for arc quenching simulation and its sudden ignition.

of fault current should be calculated then having the absolute values of fault current and the constant value of V_{arc} (which is different in two half cycles), two constant values (in two positive and negative half cycles) of conductance G can be obtained. Procedures of calculating fault current absolute value and constant G have been shown in Fig. 15 and Fig. 16. In Fig. 15, the first block called f(u) is located in control library. This block

multiplies two variable inputs of *V* and *g_calc* which are the arc voltage and the arc conductance respectively. Therefore, block output is equal to arc current (*i_calc*). Consequently, the absolute value of input current is calculated by using the another f(u) block.

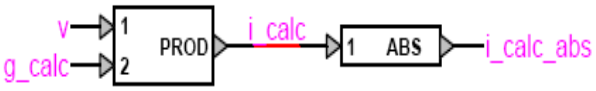

Fig. 15 Calculation of fault current absolute value.

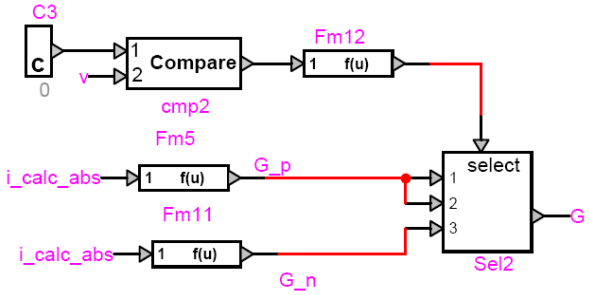

Fig. 16 Calculation of *G* constant value in two half cycles (positive and negative).

A method is used in Fig. 16 to calculate two distinct values for *G*. At first, the arc voltage and the constant value, zero, are compared with each other using a comparer. If the voltage is greater than zero, comparer output will be equal to 1, if the voltage is zero, the output will be zero and if the voltage is smaller than zero, the output is added with the value 2 which causes to changing the possible output values to 1, 2 and 3. Output of this element enters to the next element as a selector signal.

The main block which selects two values of G in two half cycles is the "input selector" located in control library of EMTPWorks. The output of this block is equal to one of three inputs regarding the control signal. It means that if the control signal value is equal to 1, output equals to input1, and if the control signal value is equal to 2, output equals to input2 and so on. In Fig. 16, for voltage values greater than or equal to zero, *G* is equal to *G_p*, and for negative voltage values, *G* equals to *G_n*. *G_p* and *G_n* are calculated through $G = |i| / V_{arc}$. In addition, to determine two constant values, *V_arc_p* and *V_arc_n* which are the inputs of program, a f(u) block is used.

According to Fig. 12, after calculating *G*, the arc conductance (*g_calc*) and its time constant (τ) can be obtained. The method of calculating time constant has been illustrated in Fig. 17.

As the constants *A*, *B* in equation $\tau = Ae^{Bg}$ have two different values in two half cycles, (*A-p* , *B-p* for positive half cycle and *A-n*, *B-n* for negative half cycle), the same approach as in calculating *G*, is used here. It should be noted that these four constant values are inputs of the model.

Finally, the most important step in simulation of HIF arc model is calculation of the arc conductance (*g_calc*). According to Fig. 13, the arc conductance by a controllable integrator (TACS type-58 integrator) located in control device of TACS library can be calculated. Therefore, two control signals of this integrator should be made at first. Actually, RES signal is the arc resistance at quenching time. Also, the control signal CTR is the same in Fig. 14. The implementation methods of RES and control signal have been shown in Fig. 18 and 19 respectively. In Fig. 20, GES signal is the inverse form of RES signal. Because the integrator output should be calculated at quenching time, output should be equal to fault conductance.

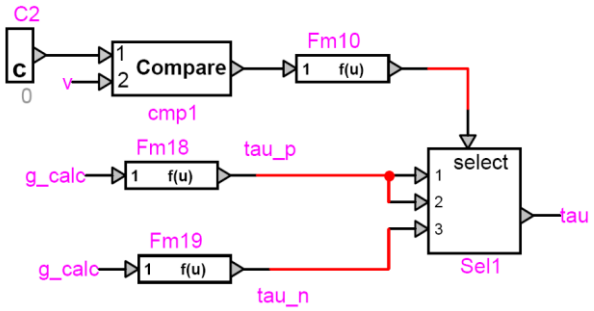

Fig. 17 Calculation of time constant.

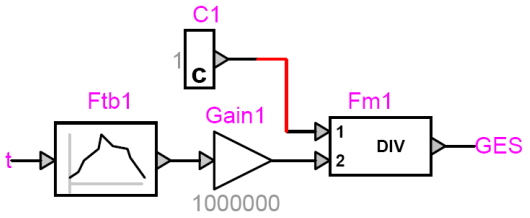

Fig. 18 Arc conductance calculation at its quenching time.

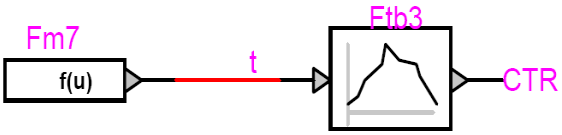

Fig. 19 Creation approach of integrator control signal.

In Figs. 18 and 19, blocks Ftb1 and Ftb3 are the table functions located in control library of EMTPWorks. Using these blocks, the output will be determined as a function of time. It means that applying some given numbers to these blocks, the control signal (in Fig. 18) and the RES signal can be created. Finally, the implementation method of arc conductance has been illustrated in Fig. 20.

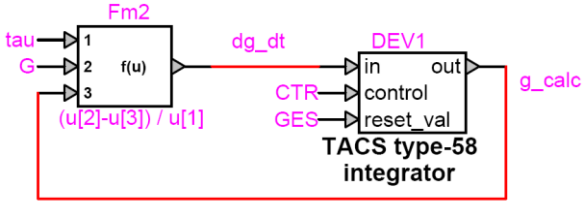

Fig. 20 *g_calc* Implementation.

As shown in Fig. 4, after measuring all the necessary quantities and in order to simulate the HIF arc model, all the circuits in a sub circuit block have been combined. In Fig. 13, the HIF element contains all the circuits shown in Figs. 15 to Fig. 20.

5. Simulation and Results

5.1 HIF characteristic

For extracting voltage-current characteristic of HIF arc, the circuit illustrated in Fig. 12 runs in EMTPWorks software. Voltage and current waveforms of HIF are sampled by scopes 1, 2 as shown in Figs. 21 and 22 respectively. In order to draw voltage-current characteristic of HIF arc, voltage waveform must be drawn based on current waveform. This characteristic has been illustrated in Fig. 23. According to Fig. 23, it is clear that HIF characteristic of two positive and negative half cycles are different. This indicates that proposed HIF arc modeling is very precise.

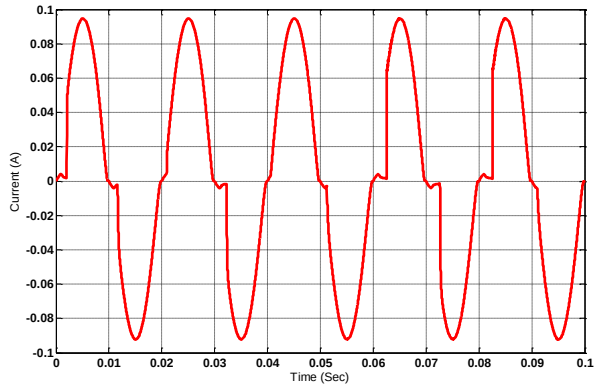

Fig. 21 Waveform of current resulted from HIF occurrence.

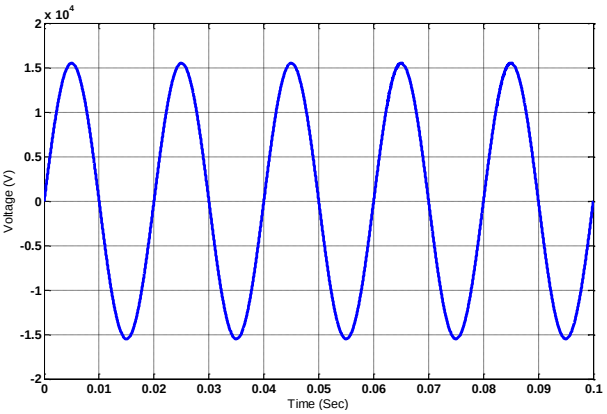

Fig. 22 Waveform of voltage resulted from HIF occurrence.

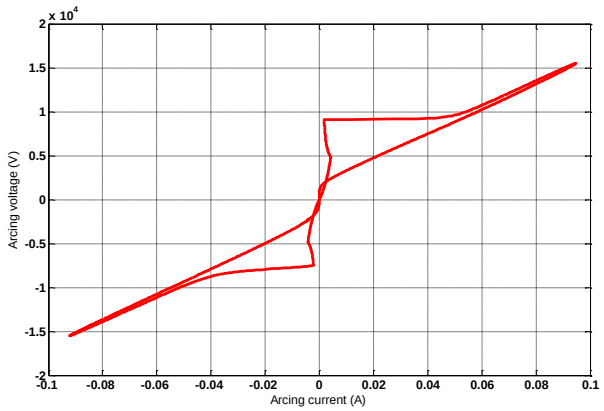

Fig. 23 Voltage-Current characteristic of HIF arc.

5.2 HIF in Distribution Network

Fig. 24 is a 20 kV unearthed distribution system simulated in EMTPWorks. The line frequency dependent model in EMTPWorks is intentionally selected to account for unsymmetrical faults. When the system and the fault modeling are combined in one arrangement, the network behavior during this fault can be investigated.

In this study, the neutral of the main transformer is isolated consistent with an unearthed system. Although this system is not intentionally connected to the earth, it is grounded by the natural phase to ground capacitances. Therefore, the fault phase current is very low allowing a high continuity of service.

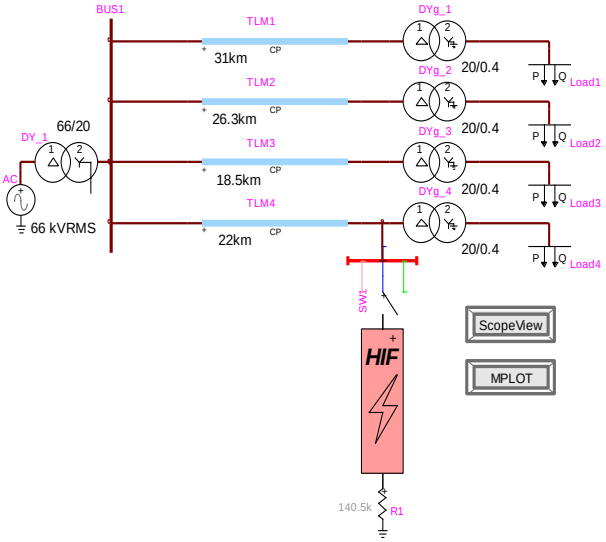

Fig. 24 Under-study distribution system used in EMTPWorks.

Fig. 25 shows HIF voltage and current waveforms in fault location of Fig. 24. The behavior of these waveforms is similar to waveforms in Figs. 21 and 22. Also, residual current waveform (sum of three phase currents) at the beginning of TLM4 has been illustrated in Fig. 26. Because of very low current value of fault, it is obvious that the behavior of single phase current waveform at the beginning of line doesn't change significantly. So this waveform is the best choice for researchers in order to extract novel approaches for HIF detection.

6. Conclusion

Unlike the other faults that lead to current with high amplitude, the fault current in HIF is very low. So the traditional protection systems like the over current protection cannot detect this fault type. Therefore, the main property of HIF is its difficult identification. Also, unsuccessful HIF detection can incur human damages or leads to firing. In order to extract a precise and appropriate approach for HIF detection, it's necessary to model high impedance fault arc. So, in this paper HIF modeling methods have been reviewed and a new method for high impedance fault modeling has been presented. The proposed method is based on N. Elkalashy et al

model. Because the arc behavior is not assumed to be the same in two positive and negative half cycles, the proposed model is more complete than the model in [20] and so it is closer to experimental results. Also, Implementation of proposed HIF arc modeling in EMTPWorks has been explained step-by-step in this paper.

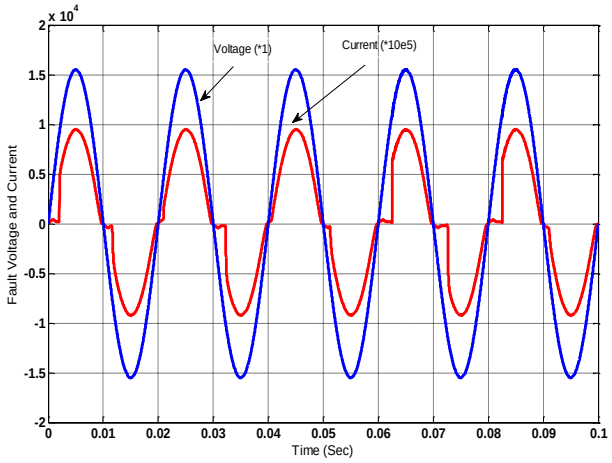

Fig. 25 Waveform of voltage and current resulted from HIF occurrence in faulted point.

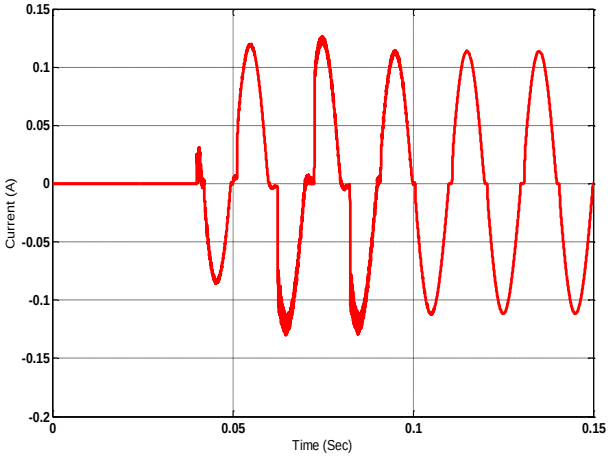

Fig. 26 Waveform of residual current resulted from HIF occurrence at the beginning of line.

7. References

[1] A. R. Sedighia, M. R. Haghifama, O. P. Malikb, "Soft computing applications in high impedance fault detection in distribution systems", Electric Power Systems Research, Vol. 76, pp. 136-144, 2005.

[2] A. S. Bretas, M. Moreto, R. H. Salim and L. O. Pires "A Novel High Impedance Fault Location for Distribution Systems Considering Distributed Generation" Transmission & Distribution Conference and Exposition: Latin America,pp. 1-6, 2006.

[3] N. Ramezani, M. Sarlak, S. M. Shahrtash and D. A. Khabori "Design and implementation of an adaptive High Impedance Fault relay" Power Engineering Conference, IPEC 2007, pp. 1131-1136, 2007.

[4] E. S. T. Eldin, D. K. Ibrahim, E. M. Aboul-Zahab and S. M. Saleh "High Impedance Faults Detection in EHV Transmission Lines Using the Wavelet Transforms" Power Systems Conference and Exposition, PES '09. IEEE/PES, pp. 1-10, 2009.

[5] T. Cui, Xin Dong, Z. Bo and S. Richards "Integrated scheme for high impedance fault detection in MV distribution system" Transmission and Distribution Conference and Exposition: Latin America, IEEE/PES, pp. 1-6, 2008.

[6] E. S. T. Eldin, D. K. Ibrahim, E. M. Aboul-Zahab and S. M. Saleh "High impedance fault detection in mutually coupled double-ended transmission lines using high frequency disturbances" Power System Conference, MEPCON 2008. 12th International Middle-East, pp. 412-419, 2008.

[7] C. J. Kim and B. D. Russell "A learning method for use in intelligent computer relays for high impedance faults" IEEE Transactions on Power Delivery, Vol. 6, pp. 109-115, 1991.

[8] S. R. Samantaray, B. K. Panigrahi and P. K. Dash "High impedance fault detection in power distribution networks using time-frequency transform and probabilistic neural network" IET Generation, Transmission & Distribution, Vol. 2, pp. 261-270, 2008.

[9] M. Sarlak and S. M. Shahrtash "High impedance fault detection in distribution networks using support vector machines based on wavelet transform" Electric Power Conference, EPEC 2008. IEEE Canada, pp. 1-6, 2008.

[10] T. M. Lai, L. A. Snider and E. Lo "Wavelet transform based relay algorithm for the detection of stochastic high impedance faults" Electric Power Systems Research, Vol. 76, pp. 626-633, 2006.

[11] M. Aucoin, Status of high impedance fault detection, *IEEE T-PAS-104, n. 3*, 1985, pp. 638-643.

[12] A. E. Emanuel, D. Cyganski, J. A. Orr, S. Shiller, E.M. Gulachenski, High impedance fault arcing on sandy soil in 15 kV distribution feeders: contributions to the evaluation of the low frequency spectrum, *Power Delivery, IEEE Transactions on , vol. 5, n. 2* , April 1990, pp.676 –686.

[13] A. M. Sharaf, L.A. Snider, K. Debnath, A neural network based back error propagation relay algorithm for distribution system high impedance fault detection, *Advances in Power System Control, Operation and Management, 2nd International Conference on* , 1993, pp. 613 –620.

[14] D. Chan, T. Wai, X. Yibin, A novel technique for high impedance fault identification, *Power Delivery, IEEE Transactions on, vol. 13, n. 3*, July 1998, pp. 738 –744.

[15] S. R. Nam, J. K. Park, Y. C. Kang, T. H. Kim, A modeling method of a high impedance fault in a distribution system using two series time-varying resistances in EMTP, *Power Engineering Society Summer Meeting, 2001. IEEE, vol. 2, 15-19* July 2001, pp. 1175 – 1180.

[16] T. M. Lai, L. A. Snider, E. Lo, Wavelet Transform Based Relay Algorithm for the Detection of Stochastic High Impedance Faults, *International Conference on Power System Transient, in New Orland*, IPTS 2003, pp.1-6.

[17] Y. Sheng, S. M. Rovnyak, Decision Tree-Based Methodology for High Impedance Fault Detection, *Power*

Delivery, IEEE Transactions on, vol. 19, n. 2, April 2004, pp. 533 – 536.

[18] M. MICHALIK, W. REBIZANT, M. LUKOWICZ, S.-J. LEE, KANG, Wavelet Transform Approach to High Impedance Fault Detection in MV Networks, *Proceedings of the 2005 IEEE PowerTech Conference*, June 2005.

[19] M. Michalik; et al, High-Impedance Fault Detction in Distribution Networks With Use of Wavelet-Based algorithm, *IEEE Transactions on Power Delivery, vol. 21, n. 4*, Oct. 2006, pp.1793-1802.

[20] N. Elkalashy, M. Lehtonen, H. Darwish, M. Izzularab, A. Taalab, "Modeling and experimental verification of a high impedance arcing fault in MV networks". IEEE TRANSACTION ON DIELECTRIC AND ELECTRICAL INSULATION, Vol. 14, No. 2, pp. 375-383, 2007.

[21] L. Eslami and R. Keivanian, "Precise Modeling and Detection of High Impedance Faults in Microgrid System Based on Residual Current Harmonic Analysis" International Review of Electrical Engineering (IREE), vol. 7, No. 1, pp. 3523-3531, 2012.